National and Kapodistrian University of Athens
Departure of Geochemistry and Economic Geology

HELLENIC REPUBLIC
National and Kapodistrian
University of Athens

BSc Thesis

Huntite-Hydromagnesite, Brucite and Dawsonite application as fire retardant fillers.

Author: Keli Ysilda

A.M.:1114201500044

Supervisor: Professor Stamatakis Michael

Athens, February 2021

Acknowledgements

I wish to extend my special thanks to my research project supervisor, Professor Stamatakis Michael for his professional guidance and valuable support and to PhD candidate Aspiotis Konstantinos for his contribution, as well as his useful and constructive comments on the present study. Also, I would like to thank the company AGROMAG, Combined Magnesium Fertilizer, Russia, and SIBELCO, Kozani, for providing me the sample studied. Furthermore, special thanks should be given to the National Kapodistrian University of Athens, National Technical University of Athens, Imerys Industrial Minerals and TITAN Cement Company S.A. for their valuable technical support and all the technicians who helped me in handling the instruments. Last, but not least, I would like to thank my family, my colleagues and friends for supporting me and encouraging me.

Table of Contents

Περίληψη

Αντικείμενο της εργασίας, είναι η διερεύνηση της θερμικής συμπεριφοράς των ορυκτών Βρουσίτη, Ντοσονίτη και μείγματος Χουντίτη – Υδρομαγνησίτη με σκοπό την πιθανή χρήση αυτών ως επιβραδυντές φλόγας. Η προέλευση των δειγμάτων ήταν αντίστοιχα από Ρωσία (AGROMAG), Αλβανία κι Ελλάδα (SIBELCO - Κοζάνη). Τα υπό εξέταση υλικά διερευνήθηκαν ποιοτικά, μέσω των τεχνικών περιθλασιμετρίας ακτίνων Χ(X.R.D.) και ηλεκτρονικής μικροσκοπίας σάρωσης (S.E.M.). προκειμένου να διασαφηνιστεί ο ορυκτολογικός προσδιορισμός και να απεικονιστεί τόσο η μορφολογία, όσο και ο χημισμός των δειγμάτων. Ακολούθως, κάθε δείγμα μελετήθηκε μέσω της θερμικής μεθόδου της θερμοσταθμικής ανάλυσης (TG-DTA) για τον προσδιορισμό της θερμικής τους αποικοδόμησης. Η θερμική ανάλυση πραγματοποιήθηκε σε αδρανή ατμόσφαιρα με τη χρήση των αερίων He, Ar και N_2 με ρυθμό αύξησης θερμοκρασίας 20 °C/min, 10 °C/min και 10 °C/min αντίστοιχα. Τα αποτελέσματα αξιολογήθηκαν σύμφωνα με την υπάρχουσα βιβλιογραφία, πραγματοποιώντας μεταξύ τους σύγκριση, ενώ στη συνέχεια συγκρίθηκαν με το επιβραδυντικό φλόγας ΑΤΗ ($Al(OH)_3$). Συμπερασματικά, από τα τρία υλικά που μελετήθηκαν, ο Ντοσονίτης παρουσίασε εφάμιλλές ιδιότητες με εκείνες του ΑΤΗ, με τη θερμοκρασία αποικοδόμησης του να βρίσκεται αρκετά κοντά σε εκείνην του ΑΤΗ, σε σχέση με τα υπόλοιπα δύο δείγματα. Επιπλέον, προτάθηκε το μείγμα Χουντίτη – Υδρομαγνησίτη να εμπλουτιστεί σε Υδρομαγνησίτη, ώστε να καλύπτεται μεγαλύτερο θερμοκρασιακό εύρος τιμών και να μπορεί να αντικαταστήσει την χρήση του ΑΤΗ. Τέλος, ο Βρουσίτης προτείνεται για χρήση σε υλικά που επεξεργάζονται σε υψηλότερες θερμοκρασίες από εκείνες που καλύπτει το ΑΤΗ.

Λέξεις Κλειδιά: Επιβραδυντικά φλόγας, Χουντίτης, Υδρομαγνησίτης, Βρουσίτης, Ντοσονίτης

Abstract

This study aims to determine the thermal behavior of the minerals Brucite, Dawsonite and the mixture of Huntite-Hydromagnesite, in order to investigate their possible use as fire retardant fillers. The Brucite sample has been received from Russia (AGROMAG), the Dawsonite sample from Albania and the mixture of Huntite-Hydromagnesite from Kozani, Greece (SIBELCO). The identification of the mineral phases, the composition and the morphology of the test materials, were conducted by the X-Ray Diffraction method (X.R.D.) and Scanning electron Microscopy (S.E.M.). Afterwards, the thermal decomposition of each sample was determined by Thermogravimetric Analysis (TGA), Differential Thermal Analysis (DTA) and Differential Scanning Calorimetry (DSC). The thermal analysis took place under He, Ar and N_2 atmosphere and heating rate of 20 °C/min, 10 °C/min και 10 °C/min, respectively. The results were evaluated according to the bibliography and compared both to each other and to the widely used fire retardant filler ATH ($Al(OH)_3$). In conclusion, of the three materials studied, Dawsonite showed properties comparable to those of ATH, as its decomposition temperature is very close to the decomposition temperature of ATH, compared to the other two materials studied. Moreover, it is proposed that the mixture of Huntite-Hydromagnesite is enriched by Hydromagnesite, in order to replace the use of ATH as a fire-retardant filler, since it can cover a wider temperature range. Finally, it is proposed that Brucite can be used as a fire-retardant filler in materials processed at higher temperatures than those where ATH is used.

Keywords: Fire-retardants, Huntite, Hydromagnesite, Brucite, Dawsonite

Chapter 1 – Introduction

In recent years, due to the worldwide demand of materials for fire retardant applications, there is need for innovative and environmentally friendly solutions that provide variety of properties and uses. A very significant factor that affects the selection of the proper fire retardant for every single use is the environmental factor. It is of a great importance that the materials that are used as fire retardants do not burden the environment. Various studies have been conducted into mineral's use as fire retardant fillers, as they occur naturally and do not emit hazardous gases during combustion. These studies have found that Hydromagnesite - $Mg_5(CO_3)_4(OH)_2 4H_2O$ and Huntite - $Mg_3Ca(CO_3)_4$, as well as Brucite - $Mg(OH)_2$, are minerals that could be used as fire retardant fillers, since their thermal decomposition can be compared to the widely used fire retardant material, Alumina trihydrate - $Al(OH)_3$. The thermal decomposition properties of a mixture of Huntite-Hydromagnesite, the mineral Brucite and Dawsonite - $NaAlCO_3(OH)_2$, a mineral which is not proposed for this use yet, have been investigated in this study. These three materials were received by SIBELCO (Kozani), AGROMAG (Russia) and Koman region (Albania), respectively. Their thermal properties were investigated and compared to the bibliography, since they are of great interest in terms of their use as fire retardant fillers.

Chapter 2 – Fire retardants

The role of fire retardants is to enhance the fire safety level of flammable materials, like polymers and plastics, by protecting them against initiating fires. The rate of decomposition of the polymer is slowed down due to the heat absorbed by the decomposing additive material and the released water dissolves the decomposition products of the flammable polymer. The flame-retardant material residue can act as a thermal border to the further decomposition of the subjacent polymer, as well.

There are two types of flame retardants, the reactive and the additive flame retardants. The first type is built chemically into the polymer molecule with the other initial constituents. On the contrary, the additive flame retardants are integrated in the plastic, either before, during, or, more frequently after polymerization. However, there can be a combination of those types, which leads to three effects, the additive, the synergistic and the antagonistic effect. The additive effect is the summation of the individual actions of those two types, while the synergistic effect is higher than this summation and the antagonistic effect is lower than this summation [1].

Nowadays, the additive type of fire retardants is mostly used. A very significant part of the additive flame-retardant market consists of fire-retardant fillers [1]. The term "fire retardant fillers" refers to products which decompose endothermically and can act as fire retardants on their own, without adding in other additives [2].

Fire-retardant fillers function by endothermic decomposition, with release of water and/or carbon dioxide, which inhibits thermal feedback [2]. [The temperature of the decomposition must be above the polymer processing temperature, but close to the polymer degradation temperature [2-4].

Nevertheless, a candidate material should have the following properties to be considered successful for commercial use. First, there must be a significant endothermic decomposition, resulting in the release of considerable amounts of water and/or carbon dioxide near to those where the host polymer decomposes (150-400°C). Secondly, it is very important to be easily processed into small particle sizes capable of giving high filler loadings. Also, it must have low solubility, low toxicity and no color. Moreover, it should have low levels of soluble impurities and extractable salts. And lastly, the most important property is low cost and ready availability [2-4].

Chapter 3 – Current Flame-Retardant Industry

The flame-retardant market consists of materials based on substances containing halogens like chlorine or bromine, nitrogen, phosphorous, antimony and metal salts and hydroxides [1, 3, 4].

The dominant materials that are used as fire retardant fillers are alumina trihydrate, ATH - $Al(OH)_3$, and magnesium hydroxide, MH - $Mg(OH)_2$. These materials constitute more than 50% by weight of the world fire retardant fillers market. They both are mostly used because they best fulfill the properties outlined above, mainly with regards to cost [2].

Specifically, $Al(OH)_3$ is less expensive than $Mg(OH)_2$ and its use is limited to polymers that are processed in the range between 200°C and 300°C, as the decomposition of ATH starts approximately at 200°C. The thermal decomposition of alumina trihydrate is represented by the following reaction:

$$2Al(OH)_3 \rightarrow Al_2O_3 + 3H_2O \text{ [2]}$$

On the other hand, $Mg(OH)_2$ is the second most widely used material in the fire-retardant industry, especially because it is more expensive than $Al(OH)_3$. As regards to the decomposition temperature, MH is stable above 300°C and decomposes at approximately 330°C. The following reaction show the thermal decomposition of magnesium hydroxide:

$$Mg(OH)_2 \rightarrow MgO + H_2O \text{ [2]}$$

These two materials are considered effective since they both decompose endothermically and decrease the possibility of fire, because of the significant release of water resulting into a large consumption of heat [2].

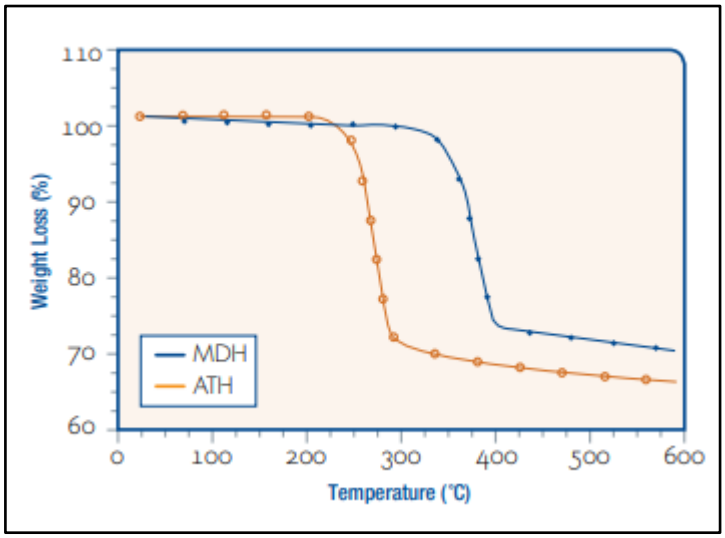

Fig. 1. TGA graph of ATH and MH.[5]

Fig.1. shows the thermogravimetric analysis of alumina trihydrate compared to magnesium hydroxide's thermal decomposition. It is obvious that MH decomposes at higher temperatures than ATH [5], making it suitable for use in materials processed at higher temperatures.

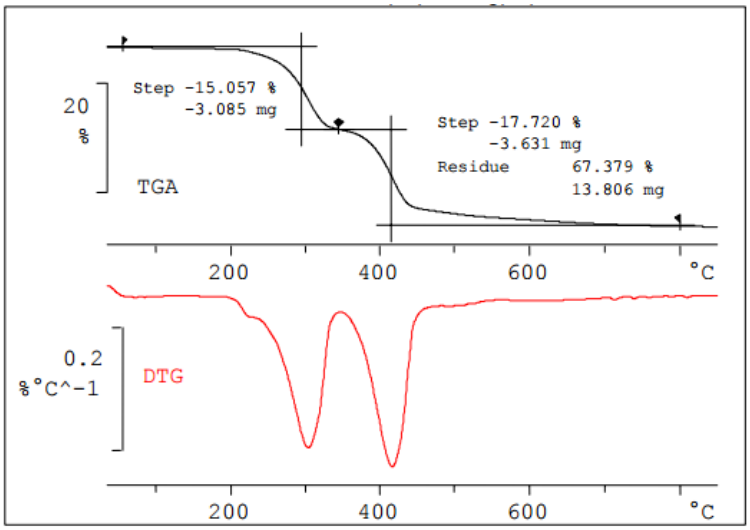

Fig. 2. TGA of a mixture of $Al(OH)_3$ and $Mg(OH)_2$. [6]

Fig.2 displays the TGA (black) and the DTG (red) curves of a mixture of ATH and MH as a function of temperature. The first bigger point of inflection at about 300°C refers to the decomposition of alumina trihydrate, where the elimination of the water takes place.[18] At the second big point of inflection at about 415°C, the elimination of the water from magnesium hydroxide occurs [6].

Other materials, that meet most of the requirements to be considered efficient flame-retardant fillers, are Basic Magnesium Carbonates (Hydromagnesite – $4MgCO_3 \cdot Mg(OH)_2 \cdot 4H_2O$), Boehmite- AlO(OH), and Calcium Sulphate Dihydrate (Gypsum – $CaSO_4 \cdot 2H_2O$). Calcium carbonate fillers, either natural or synthetic, are also in use in elastomers and PVC. All these materials are effective, but in comparison to the ATH and MH, there should be used larger quantities to obtain the same performance levels [2].

In conclusion, ATH and MH have an assured role in flame retardancy, but there is need of innovative and progressive inventions that provide solutions and variety for different requirements of this industry.

Chapter 4 – Geological setting

The first mineral that was studied, is a mixture of Huntite-Hydromagnesite. It has white color and was received as a powder of a natural sample, which was extracted from the Neraida area, Kozani, northern Greece, where it is commercially exploited by the company SIBELCO SA. Huntite-Hydromagnesite mixture is a processed material produced by two quarries located on the southeast side of the city of Kozani. These two deposits have a thickness of about 4m and more than 500.000 tons stocks. The main quarry which exploits this material is called "Neraida" and is covered by dolomitic claystone. This product occurs in the Late Neogene sedimentary rocks, which constitute the uppermost succession of the Kozani basin and have an approximate thickness of about 100m[3]. These stratigraphically uppermost sediments lie directly on the Mesozoic carbonate basement, which consists of dolomitic marbles and limestones.

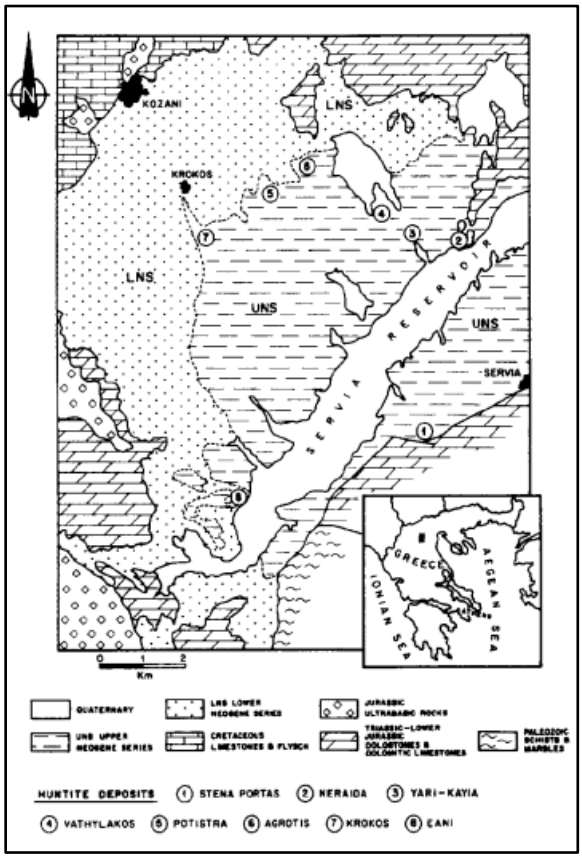

Fig. 3. Schematic geologic map of Huntite-Hydromagnesite quarries, Kozani. [7]

Macroscopically, Hydromagnesite is detected in the Huntite as asymmetrical modules up to 5cm size, whereas Huntite is observed as spherical or platy modules, with a

maximum thickness of about 15cm, in claystone, or as a mixture with magnesite deposited on the Mesozoic carbonate basement [8, 9].

The final product has undergone drying, grinding and air-classification in order to remove any larger grain sized granules of aragonite or magnesite, which are found with the raw material [8].

In Fig.3 a schematic geological map of the Kozani Basin with location of the huntite/hydromagnesite deposits is shown: 1. Stena Portas, 2. Neraida, 3. Yiari-Kayi, 4. Vathylakhos, 5. Potistra, 6. Agrotis, 7. Krokos, 8. Eanl. The Neraida deposit is the source of the sample that was studied [7].

Fig. 4. A quarry face of Huntite-Hydromagnesite at Lefkara-Neraida quarry, Kozani. Picture from M. Stamatakis 2019.

In Fig.4, the deposition of Huntite-Hydromagnesite at Lefkara-Neraida is depicted. The snow-white mineral assemblages is a mixture of Huntite-Hydromagnesite which contains minor aragonite and magnesite, covered by a low in thickness dolomitic limestone layer [8].

The second mineral that was studied, is Brucite originated from Russia. This mineral of white color is extracted from Kuldur deposit, a Brucite ore which provides high chemical purity products and is in Obluchensky district in Jewish Autonomous Region, Russia [10].

The Kuldur deposit involves two ores, the Main and the Southern. It is mined by the open pit method, under explosion. The amount of the resources is estimated about 7 million tons. The ore is hosted by low Cambrian schists and is in contact with silicate

carbonate rocks and ophicalcites. In particular, the mineral body is dissected by bostonite dikes and Upper Paleozoic dioritic porphyries. Moreover, under the brucite ore, Late Cretaceous age crouans lay in direct contact. Those crouans were the source of heat at the primary underplayed magnesite which was reconverted into brucite.

The final product is available for industrial use after enrichment, crushing and classification [10].

Fig. 5. Kuldur deposit of Brucite, Russia. [10]

In Fig.5, the Kuldur deposit is shown, where Brucite is exploited and after enrichment, crushing and classification is available as a commodity [10].

The third mineral studied, is Dawsonite ($NaAlCO_3(OH)_2$), a white mineral originated from Koman, in northern Albania.

The samples of Dawsonite were taken from a deposit located about 15km north of the town Puka along the course of the river Drin. Dawsonite deposit appears as a horizon 500x100m with thickness at about 20m and lies within carbonate-rich layers [11].

The main occurrences of Dawsonite are within argillaceous schists, marlstone, carbonate rocks and sandstone formations of the upper Cretaceous to Lower-Middle

Paleogene. These lithologies are related to two forms of occurrences, 1) dawsonite associated with realgar orpiment and 2) dawsonite as the only ore mineral. The deposit where the samples were taken from, is not a mined ore, but the estimated potential reserves of dawsonite are 2x106 tons at 10–15% average grade in the carbonate wall rocks, and 5x106 tons at 5% average grade in the sandstone occurring in the Xhan Flysch formation (Borova et al. 1991) [11].

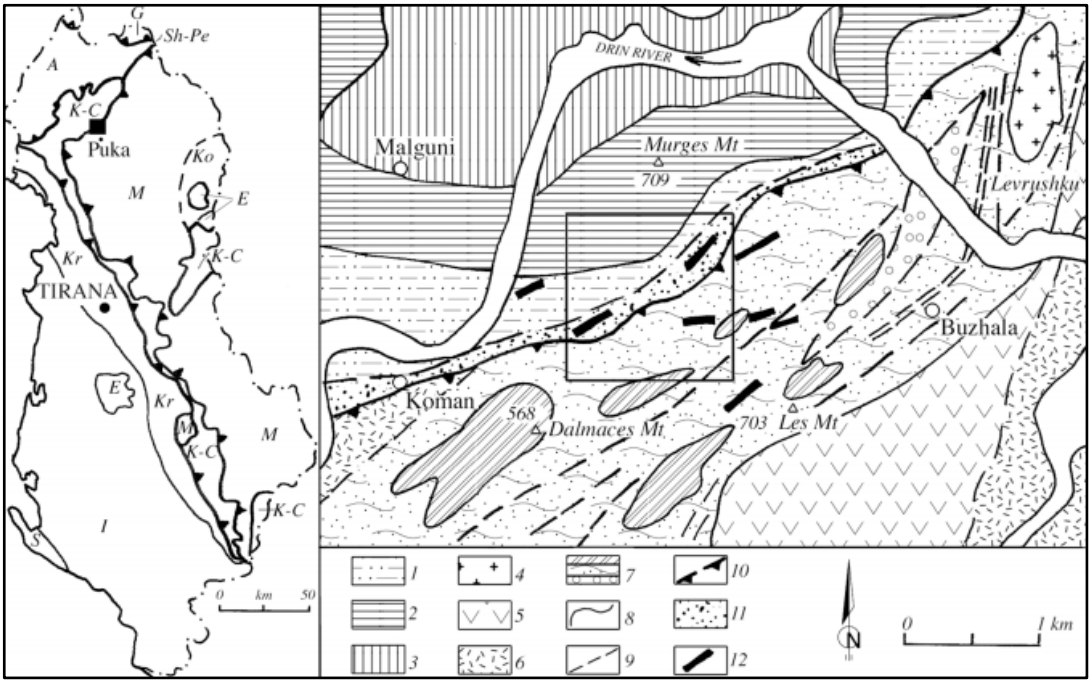

Fig. 6. Geological sketch-map of Koman region. [11]

Fig.6 shows the geological zones that appear at the Koman region.
Krasta–Cukal zone: 1) Upper Cretaceous – Lower-Middle Paleogene Flysch, 2) Upper Cretaceous limestone, 3) Upper Jurassic – Lower Cretaceous cherty limestone, Mirdita zone: 4) Jurassic? Cretaceous? granite, 5) Triassic–Jurassic volcano-sedimentary series, 6) Jurassic ophiolitic formation, 7) Triassic limestone and argillaceous schists with lenses of silex, 8) stratigraphic boundaries, 9) faults, 10) overthrusts, 11) zone of realgar–orpiment and dawsonite mineralization, 12) mineralized bodies [11].
Square area of Fig 5. tectonic sketchmap of Albania (simplified from Shallo et al. 1985) showing location (black rectangle) of study area. Tectonic zones: Ko: Korrab; G: Gash; M: Mirdita; K–C: Krasta–Cukal; Kr: Kruja; I: Ionian; S: Sazan; E: evaporite diapirs; A: Alps. Sh–Pe: Shkodra–Pec tectonic alignment [11].

Fig. 7. Picture of Dawsonite from the Koman region.

Fig. 8. Picture of Dawsonite from the Koman region.

Fig.9. Image of Dawsonite crystals by stereo microscope.

Fig.10. Image of Dawsonite crystals by stereo microscope.

The figures 9 and 10 display the mineral Dawsonite, a low temperature hydrothermal mineral which occurs as tabular white crystals and radically concentric aggregates inside rhombs of dolomite and calcite [11].

Chapter 5 – Experimental

A. Materials

In this study three samples were chosen for investigation:

- Sample 1. Huntite-Hydromagnesite received from north Kozani, Greece.
- Sample 2. Brucite received from Agromag, Combined Magnesium Fertilizer, Russia.
- Sample 3. Dawsonite received from Koman, north Albania.

B. Instruments

The three samples were determined using an X-ray diffractometer (XRD). The analyses were conducted using an XR Diffractometer Bruker (Siemens) D5005 and the mineral identification of the resulting scans was made with the use of the program DIFFRACplus EVA (Version 10.0) at the National and Kapodistrian University of Athens.

Scanning electron microscope images were taken with a JEOL JSM 5600 scanning electron microscope at the National and Kapodistrian University of Athens.

Thermogravimetric Analysis (TGA), Differential Thermal Analysis (DTA) and Differential Scanning Calorimetry (DSC) were performed using three different models of instruments, SETARAM92-1.68 (IMERYS INDUSTRIAL MINERALS), NETZSCH Proteus Thermal Analysis (TITAN Cement Company S.A.) and METTLER TOLEDO TGA/STDA 851e (NATIONAL TECHNICAL UNIVERSITY OF ATHENS).

Stemi 1000/2000/2000-C Stereo Microscopes at the National Technical University of Athens.

C. Methods

The compositions of the three samples were conducted for the identification of the mineral phases and the compounds that are present in each one, based on the powder X-Ray diffraction analysis method. Using the powder X-Ray diffraction method, there can be determined the percentage of a compound in its solid mixture.

The samples were prepared by hand grinding with the use of an agate mortar and pestle to a fine homogenous powder. Thus, the small crystallites are oriented in every possible

direction so that when an X-ray beam passes through the material, there could be a significant number of particles oriented in such way to fulfill the condition needed. Every crystalline substance has its own unique X-Ray diffraction pattern. Thus, the identification is successful when there is found an exact match between the pattern under consideration and a standard sample [12].

The surface morphologies of the three samples were determined after preparation of the samples by graphite plating.

In terms of thermal analysis test, each sample, which were finely ground, weighed approximately 25mg ± 5mg and was put in a platinum sample holder. The sample holder was placed on a platinum thermobalance, and this system described above is mounted inside an autoclave. Each of the different types of instruments provides information about the samples through a different thermal method and analysis conditions.

Thermogravimetric Analysis (TGA) is a method used to determine the mass loss at specific temperatures. In this technique the mass of a sample in a controlled atmosphere is recorded continuously as a function of temperature or time as the sample's temperature increases. There is produced the derivative of the thermogram, which provides the information needed [12]. The instrument used at the National Technical University of Athens provides measurements using only the TGA method with temperature range of 25-1100°C, heating rate of 10°C/min and inert nitrogen atmosphere N_2 at a flow rate of 50ml/min.

The instrument used at IMERYS provides measurements using the Thermogravimetric Analysis (TGA) method and the Differential Thermal Analysis (DTA) method with temperature range of 100-1100°C, heating rate of 20°C/min and inert He atmosphere OR otherwise specified. The DTA method measures the difference between the substance's temperature and the temperature of a reference material as a function of temperature. As a result, the differential thermogram plots show the difference in temperature ΔT between the sample temperature and the reference temperature, which according to the enthalpy, are characterized as endotherm or exotherm curves [12].

The instrument used at TITAN provides measurements using the Thermogravimetric Analysis (TGA) method and the Differential Scanning Calorimetry (DSC) method with temperature range of 20-1000°C, heating rate of 10°C/min and atmosphere Ar. In DSC method the difference in the heat flow between the sample and the reference material is measured. Thus, the differences in energy are measured and endotherm or exotherm events can be indicated [12].

Chapter 6 – Results

The results of the XRD, SEM and TGA-DTA-DSC analysis are the following.

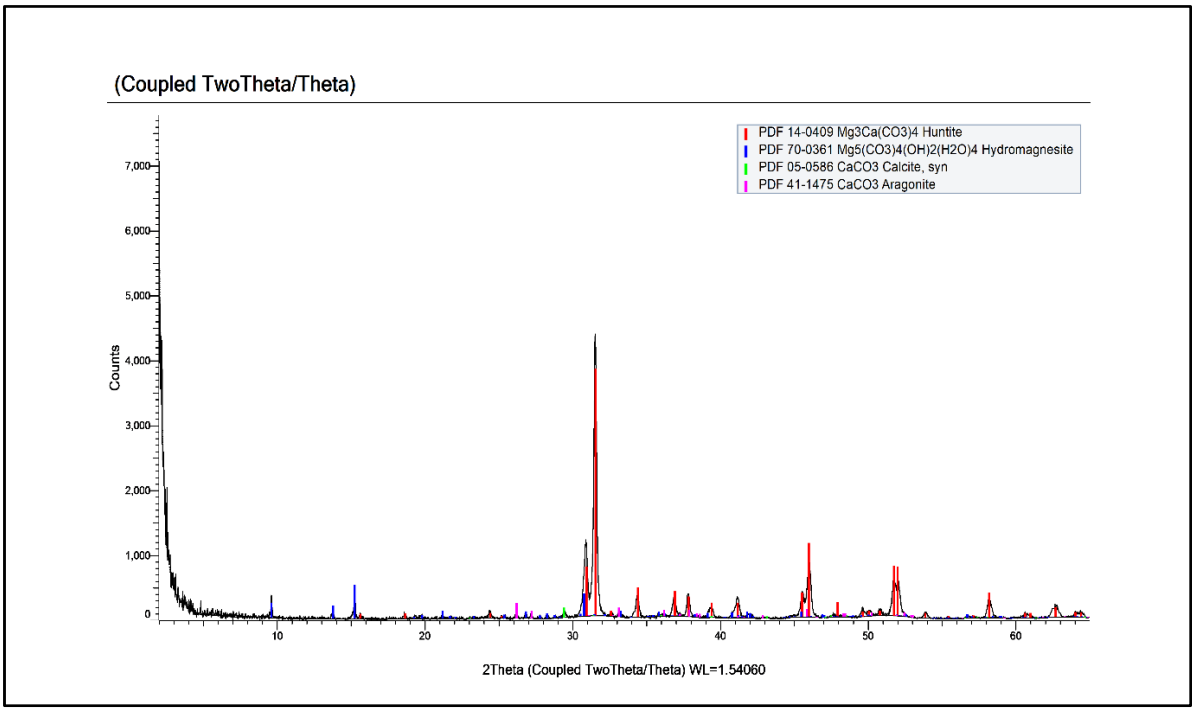

Fig.11. XRD pattern for Sample 1. Huntite-Hydromagnesite.

XRD analysis of the sample 1. Huntite-Hydromagnesite is shown in Fig.11. It is found that the basic minerals are Huntite - $Mg_3Ca(CO_3)_4$ at a rate of 88.51% and Hydromagnesite - $Mg_5(CO_3)_4(OH)_2 4H_2O$ at a rate of 8.29%. The other impurities are Aragonite at a rate of 2.19% and Calcite at a rate of 1.01%.

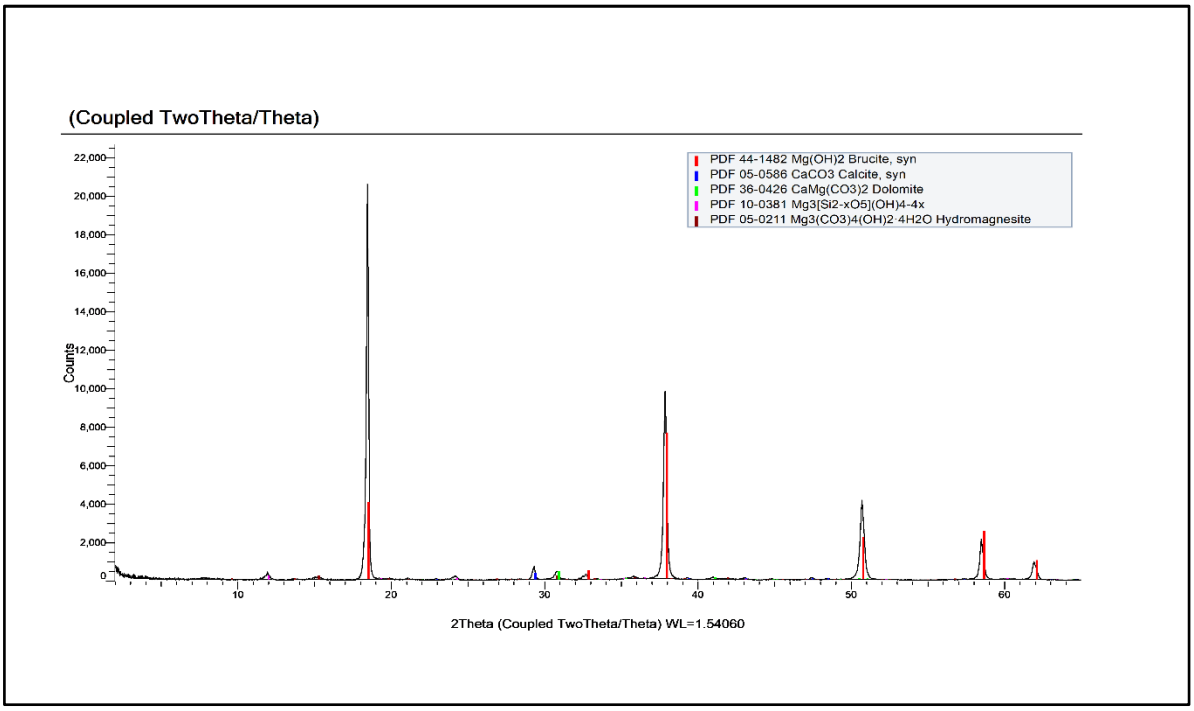

Fig. 12. XRD pattern for Sample 2. Brucite.

XRD analysis of the sample 2. Brucite is shown in Fig.12. It is found that the basic minerals are Brucite - $Mg(OH)_2$ at a rate of 82.81% and Hydromagnesite - $Mg_5(CO_3)_4(OH)_2.4H_2O$ at a rate of 5.81%. The other impurities are Calcite at a rate of 3.08%, Dolomite at a rate of 3.02% and Serpentine at a rate of 5.28%.

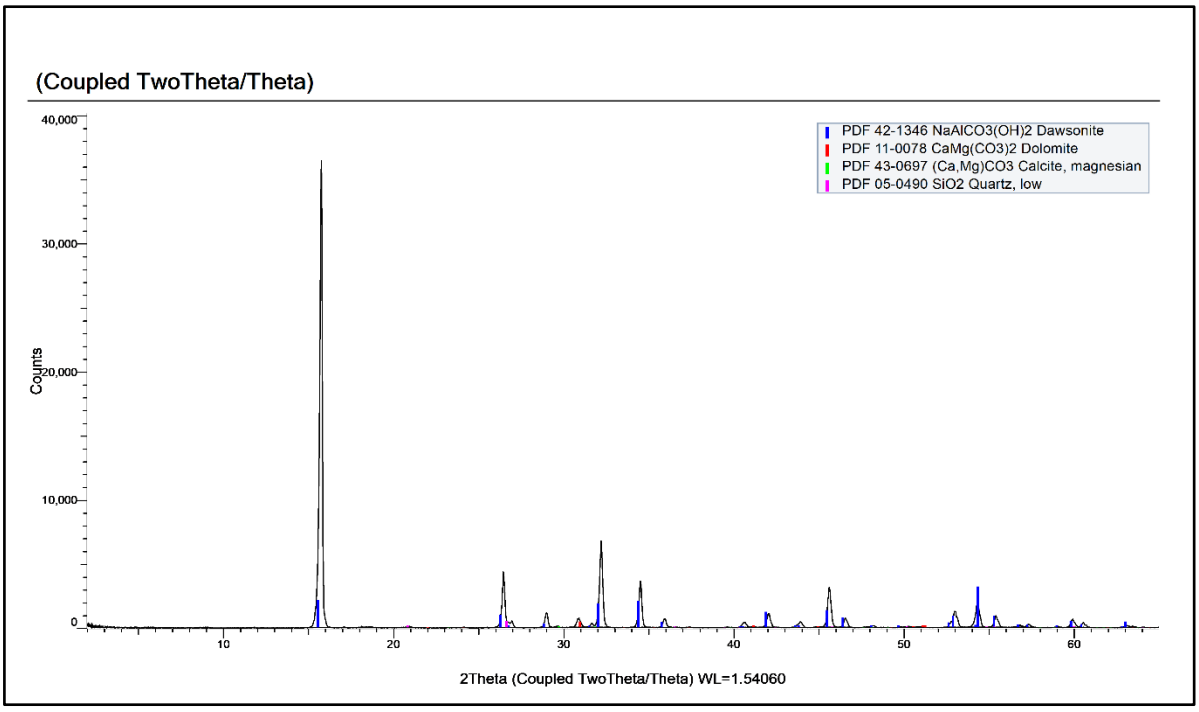

Fig. 13. XRD pattern for Sample 3. Dawsonite.

XRD analysis of the sample 3. Dawsonite is shown in Fig.13. It is found that the basic minerals are Dawsonite ($NaAlCO_3(OH)_2$) at a rate of 92.64% and Dolomite ($CaMg(CO_3)_2$) at a rate of 5.03%. The other impurities are Quartz at a rate of 1.65% and Calcite at a rate of 0.68%.

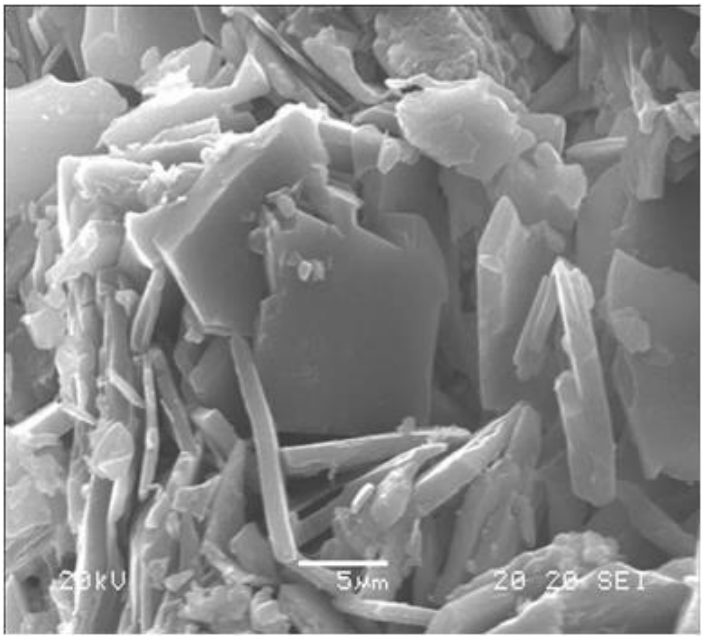

Fig. 14. Scanning electron microscopy image of Hydromagnesite blade crystals, mixed with Huntite small crystals, Neraida deposit (picture from M. Stamatakis).

Several authors have detected that in Neraida deposit, larger Hydromagnesite particles are interspersed with smaller platy huntite particles [13]. In Fig.14. the platy particles of Huntite have thickness of about 1-1.2μm and the particle of Hydromagnesite at the center of the picture has an area of 107μm^2.

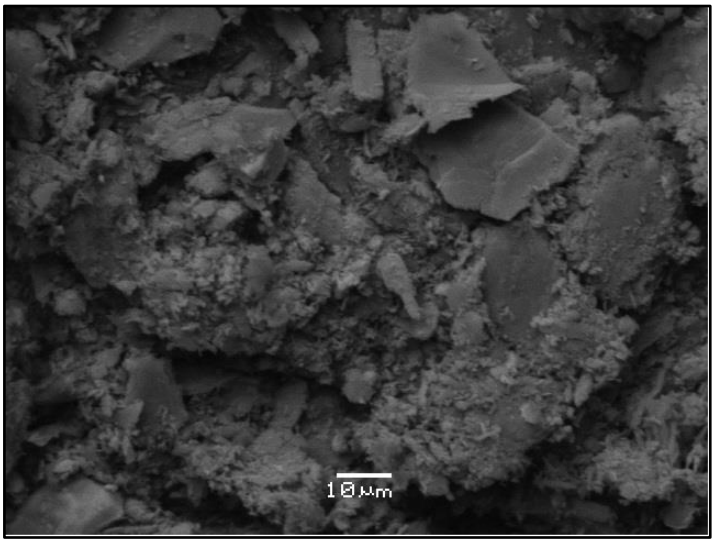

Fig. 15. Scanning electron microscopy image of Brucite powder – commercial sample (picture by Varvara Spanou, 2019).

Fig. 15. Shows the brucite crystals using the S.E.M. technique. As can be seen, the platy crystals are covered by other of smaller dimensions. The smaller particles are speculated as fragments of the bigger crystals. The platy crystals have an area of about 250-700 μm^2.

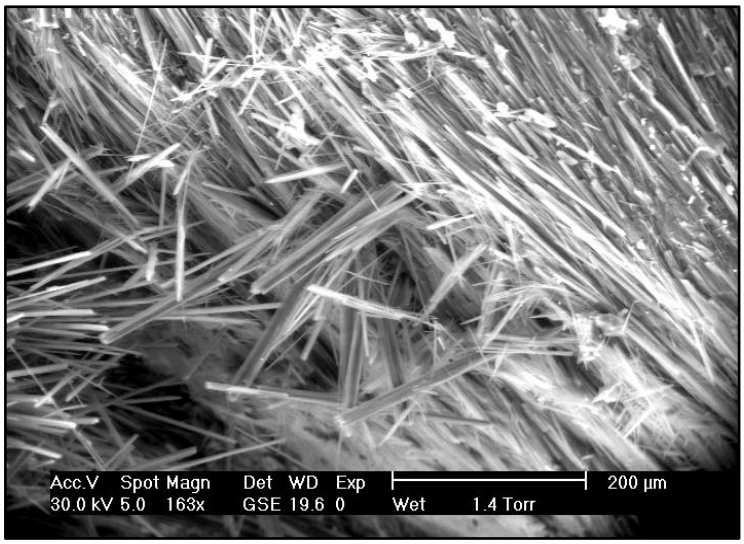

Fig. 16. Scanning electron microscopy image of Dawsonite, picture by Stamatakis, 2012.

In Fig. 16. the fibrous crystals of Dawsonite are depicted, their thickness is about 5-13µm.

The results from the three different thermal analysis methods are placed together in graphs for each of the samples that were tested.

6.1 Huntite – Hydromagnesite

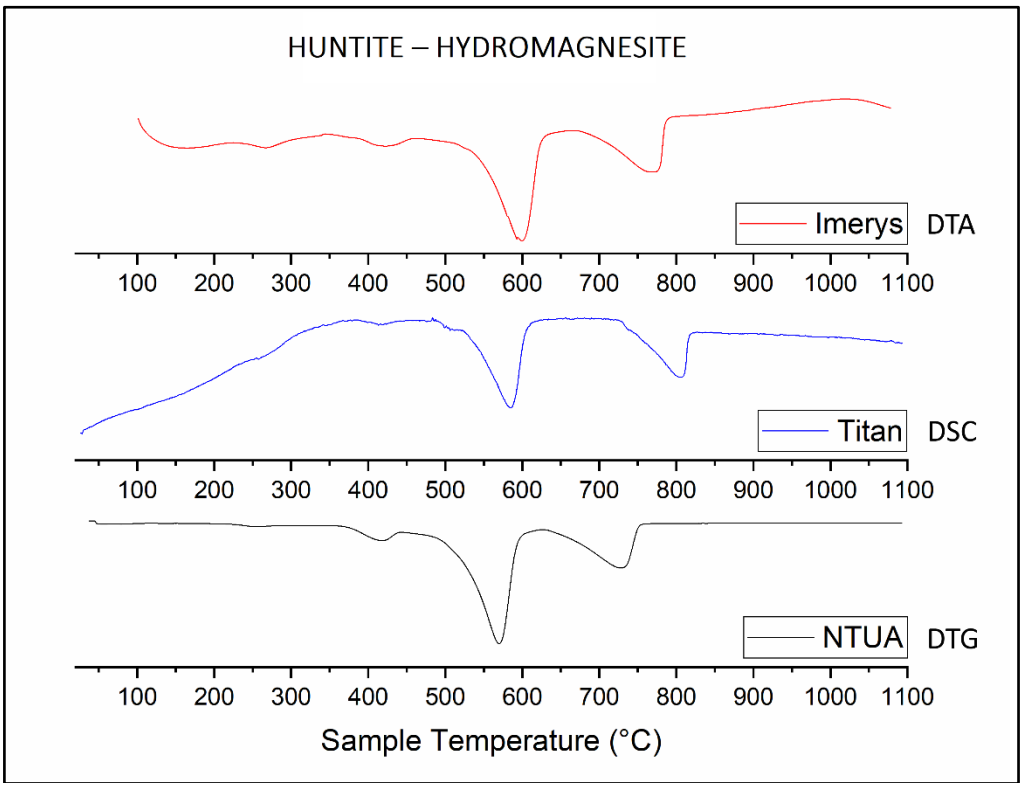

Fig. 17. TG thermograms of Sample 1. Huntite-Hydromagnesite.

The TG (DTA,DSC,DTG) curves of thermal analysis of Huntite-Hydromagnesite from the three different types of instruments are presented in Fig. 17.

The red curve was conducted from the instrument SETARAM92-1.68, using the DTA method, with temperature range: 100-1100°C, heating rate: 20°C/min and inert He atmosphere. This curve shows the wide range of decomposition of the mixture of Huntite-Hydromagnesite starting at about 250°C and being complete at about 800°C.

In particular, Hydromagnesite begins to decompose at about 250-300°C and Huntite at about 380-450°C, where the release of water of crystallisation takes place. Due to the higher content of the mixture in Huntite (88.1%) the loss of the Hydromagnesites' hydroxides as water is not clear as a separate loss in this curve. However, the release of water from decomposition of the Huntite's hydroxides is detected at about 580-600°C. The second major mass loss is detected between temperatures 725°C and 780°C, where the decomposition of the carbonate leads to release of carbon dioxide.

The blue curve was conducted from the instrument NETZSCH Proteus Thermal Analysis, using the DSC method, with temperature range: 20-1000°C, heating rate: 10°C/min and atmosphere Ar.

This curve, also, shows the wide range of decomposition of the mixture of Huntite-Hydromagnesite starting at about 380°C and being complete at about 810°C. As in the red curve, here, there is not detected the decomposition of the Hydromagnesite, since the content of Hydromagnesite in the sample is very low. Therefore, there are shown only two decomposition peaks. The first one, at about 550-590°C, where the decomposition of the hydroxides takes place and the second one, where the carbon dioxide is lost, at about 760-810°C. There must be noticed that the shape of the curve at the beginning of the graph was caused by an explosion near the laboratory, where TITAN has its own quarry.

The black curve was conducted from the instrument METTLER TOLEDO TGA/STDA 851e, using the TGA method, with temperature range: 25-1100°C, heating rate: 10°C/min and inert nitrogen atmosphere N_2 at a flow rate of 50ml/min.

As mentioned before, here there is not any detection of the decomposition of Hydromagnesite, only the three decompositions of Huntite, each one associated with peaks mentioned before. The range of the decomposition varies from approximately 400°C to 750°C. The first peak, at about 400-425°C represents the release of water of crystallization. The second, bigger peak at about 540-580°C is associated with the decomposition of the hydroxides, resulting into release of water. The third peak shows the release of carbon dioxide as a result of decomposition of the carbonates at about 725-750°C.

Comparing the information obtained by the three different curves, there is no significant deviation of the decomposition temperatures of the sample 1. Huntite-Hydromagnesite. It must be noticed though that, the little difference between the temperatures of the decomposition temperatures is due to the different conditions of atmosphere under which every model operates.

6.2 Brucite

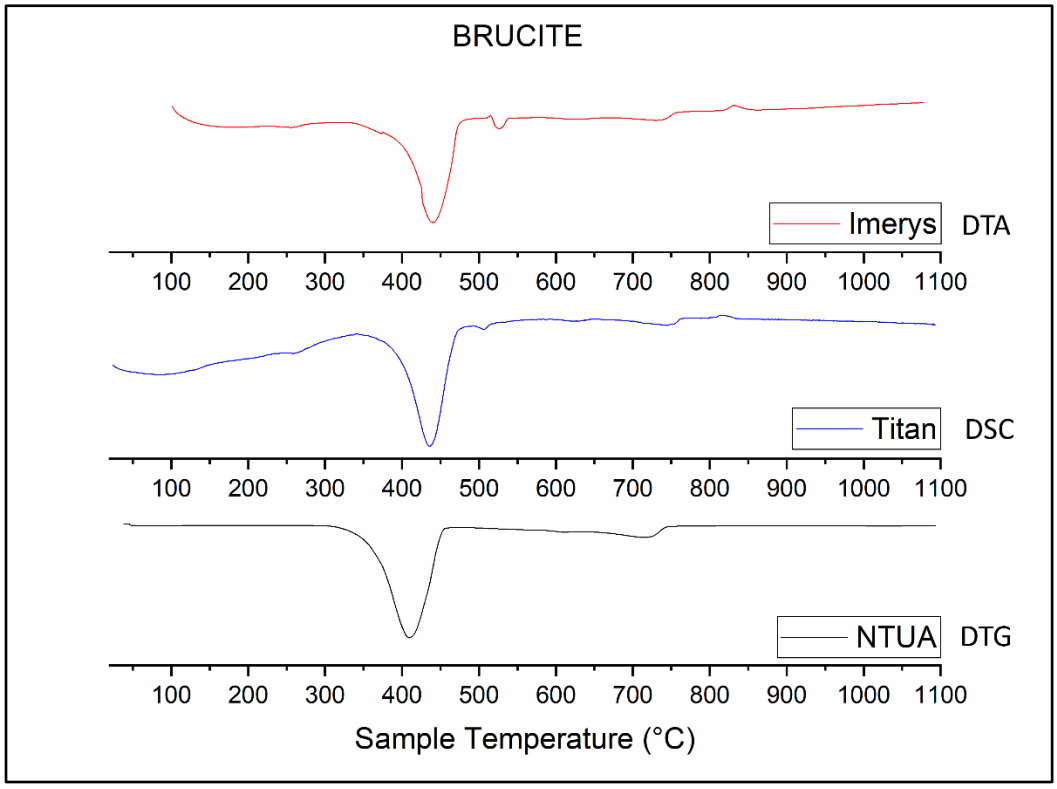

Fig. 18. TG thermograms of the Sample 2. Brucite.

The TG (DTA,DSC,DTG) curves of thermal analysis of Brucite from the three different types of instruments are presented in Fig. 18.

The red curve is characterized by a big endothermic peak and two smaller endothermic peaks. The first peak at about 400-475°C is attributed to the decomposition of $Mg(OH)_2$ to form MgO and the release of water from this decomposition. After that, there is determined a slight peak at about 525°C, which could be a result of the further decomposition of brucite and the residual water molecules from the sample [14]. At about 750°C is noticed a weak endothermic event which represents the mass loss due to the decomposition of the dolomite.

At the blue curve, there are noticed the same three peaks as the red curve, differing only at the size and the temperature of the observation of the second peak which is noticed at about 500°C, but represents again the probable further decomposition of brucite.

The black curve is characterized only by two decomposition peaks. The first and bigger one at about 350-450°C, represents the decomposition of $Mg(OH)_2$ to the formation of

MgO. The second one and smaller peak is detected at about 700-750°C and is associated to the decomposition of dolomite.

Comparing the information obtained by the three different curves, there is no significant deviation of the decomposition temperatures of the sample 2. Brucite, except the fact that at the black curve there is not noticed a peak which corresponds to the probable further decomposition of brucite. It must be noticed though, that the little difference between the temperatures of the decomposition temperatures is due to the different conditions of atmosphere under which every model operates.

6.3 Dawsonite

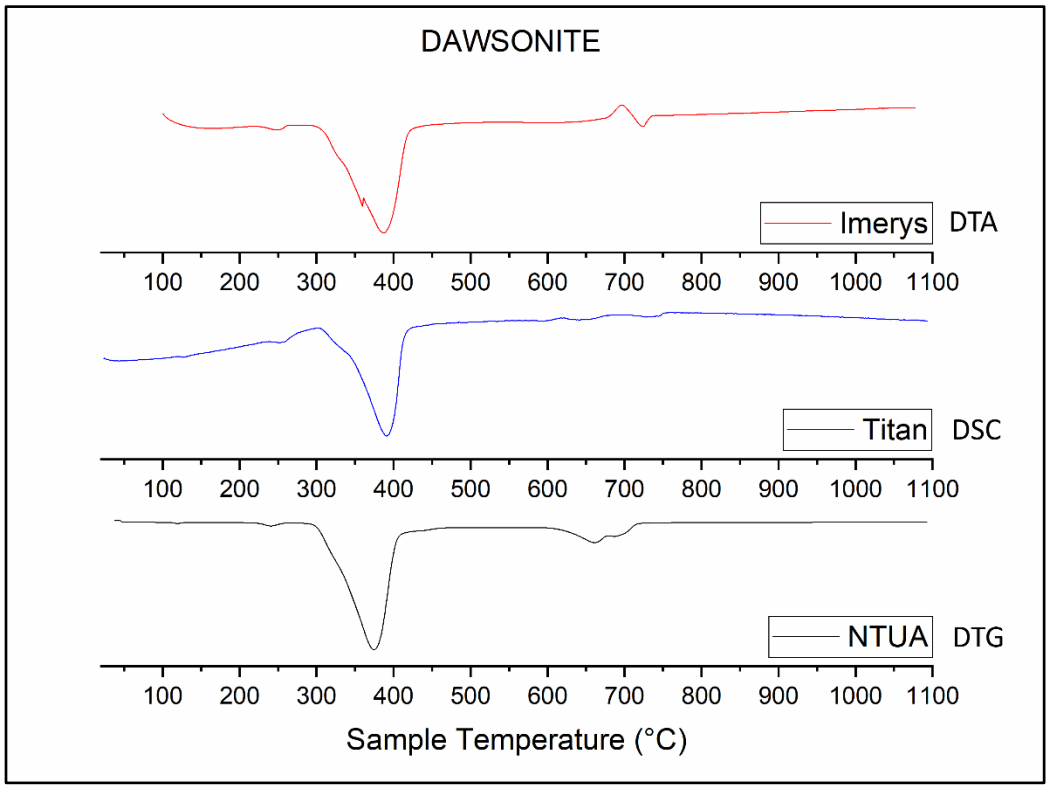

Fig. 19. TG thermograms of the Sample 3. Dawsonite.

The TG (DTA,DSC,DTG) curves of thermal analysis of Dawsonite from the three different types of instruments are presented in Fig. 19.

At the red curve are detected two endothermic peaks. The first, and more significant one, is observed at a range between 300°C and 410°C associated with the decomposition of the dawsonite mineral - $NaAlCO_3(OH)_2$.

The second one, which is very small, is associated with the decomposition of the dolomite and appears at about 700-730°C.

The blue curve has the bigger peak exactly at the same temperatures as the red one (300-410°C), which is associated with the decomposition of dawsonite. However, there is not detected the second smaller peak, which is observed at the red curve, maybe because that sample had a slight quantity of dolomite.

The black curve has a significant peak at a range between 290°C and 400°C, which represents the decomposition of dawsonite. The second and weaker peak, is detected at about 650-710°C and represents the decomposition of dolomite.

There is no significant difference between the decomposition temperatures conducted from the three different curves. The minor deviation of the peaks observed at the three curves is due to the experimental conditions of each one.

All the thermograms of the three samples (Huntite-Hydromagnesite, Brucite and Dawsonite), are characterized by a minor mass loss at the very beginning of the curves, because of the initial loss of the moisture of the minerals.

HUNTITE-HYDROMAGNESITE		BRUCITE		DAWSONITE	
Temperature (°C)	Mass Loss (%)	Temperature (°C)	Mass Loss (%)	Temperature (°C)	Mass Loss (%)
264.90 ±2.06	1.44 ±0.07	253.24 ±3.30	1.63 ±0.30	245.97 ±5.51	0.71 ±0.06
418.63 ±0.01	4.30 ±0.30	**428.78 ±11.82**	**23.60 ±0.36**	**376.43 ±2.43**	**33.68 ±0.13**
585.86 ±13.91	**29.99 ±0.09**	618.03 ±4.64	1.65 ±0.30	694.57 ±4.12	7.96 ±0.24
753.25 ±21.36	13.25 ±0.14	726.43 ±4.49	3.29 ±0.05		

Table 1. The average value of the mass losses of the three samples from the three experiments.

Table 1. shows the average values of the mass losses of the samples, as measured from the three different experiments.

Huntite-Hydromagnesite has a major mass loss at approximately 585°C which is obviously associated to the decomposition of the $Mg_3Ca(CO_3)_4$. The major mass loss

of Brucite occurs at approximately 428°C, where the decomposition of the $Mg(OH)_2$ takes place. Dawsonite shows a major mass loss at approximately 376°C where the decomposition of the $NaAl(OH)_2CO_3$ occurs.

Chapter 7 – Discussion

7.1 Huntite-Hydromagnesite

As far as concerned Huntite-Hydromagnesite, from the XRD results occurs that the concentration of Huntite in the mixture is higher than the concentration of Hydromagnesite. In particular, there is 88.51% Huntite and 8.29% Hydromagnesite. For this reason, at the TG profiles the endothermic events associated to the decomposition temperatures of Huntite will prevail over the those of Hydromagnesite, which was the result, since the endothermic curves associated to the thermal decomposition of Huntite are more distinct than those of the Hydromagnesite. According to Hollingberry and Hull, Hydromagnesite decomposes endothermically at a temperature range of approximately 220°C to 550°C. The thermal decomposition of Hydromagnesite is shown by the following reaction [15]:

$$Mg_5(CO_3)4(OH)_2.4H2O \rightarrow 5MgO + 4CO_2 + 5H_2O$$

The thermal decomposition of Huntite occurs at temperature range of approximately 450°C to 800°C according to the following reaction [15]:

$$Mg_3Ca(CO_3)_4 \rightarrow 3MgO + CaO + 4CO_2$$

At the Handbook of TGA system of minerals [16], different authors claim that Hydromagnesite decomposes at a temperature range of 296°C to 600°C. The dehydration occurs at about 296-375°C, the dehydroxylation at about 420-440°C and the decarbonation at about 530-600°C. Also, the thermogravimetric curves of Huntite, shown at the Handbook of TGA system of minerals are very similar to the curves obtained by the thermogravimetric analysis of this study. In particular, the temperature range of decomposition of Huntite is of approximately 480°C to 900°C.
The two main reactions reported are the following:

550°C – 650°C: $Mg_3Ca(CO_3)_4 \rightarrow 3MgO + CaCO_3 + 3CO_2$
800°C – 900°C: $CaCO_3 \rightarrow CaO + CO_2$

The information mentioned above does not differ significantly from the results obtained by this study for the mixture of Huntite-Hydromagnesite. Thus, at the thermographic analysis curves, as mentioned before, the occurrence of Huntite prevails the occurrence of Hydromagnesite. As a result, only the decomposition temperatures of Huntite are shown at the TG profiles. The minor differences between the temperatures obtained from this study and those obtained from the bibliography are due to the use of different instruments for the experiments.

7.2 Brucite

The decomposition temperature of Brucite according to Walter and Wajor starts at about 330°C and is represented by the following reaction [17]:

$$Mg(OH)_2 \rightarrow MgO + H_2O$$

Also, as mentioned in the Handbook of TGA [16], a sample with 22% concentration of Brucite has a decomposition temperature range of about 350-450°C.

Liu et.al (2018) [14] in their study performed thermogravimetric tests of the decomposition of Brucite that were carried out at heating rates of 5, 10, 15, 20 and 25°C min^{-1}. The decomposition had a temperature range from approximately 330°C to 410°C, and the maximum value of the mass loss occurred at 375°C. The different heating rates under which the experiments were carried out, confirm that as the heating rate increases, the decomposition temperature increases significantly.

The sample of Brucite studied in this study, according to the endothermal curves conducted from TG analysis, thermally decomposes at about 380-500°C. There is a minor difference between data, which apparently lies in the different experimental conditions.

7.3 Dawsonite

As regards to the thermal decomposition of Dawsonite, the thermoanalytic curves conducted from this study, are very similar to those mentioned in the Handbook of TGA [16]. The decomposition of Dawsonite is represented by the following reaction that occurs in four steps:

$$NaAl(OH)_2CO_3 \rightarrow NaAlO2 + H_2O + CO_2$$

The temperature range of the decomposition mentioned, is about 290-450°C with a small exothermic peak at 828°C that indicates crystallization of sodium aluminate. The major mass loss occurs at 370°C.

According to Smith and Young (1975) [18], Dawsonite decomposes at about 350°C through the following reaction:

$$2\ NaAl(OH)_2CO_3 \rightarrow Na_2CO_3 + A1_2O_3 + 2\ H_2O + CO_2$$

In this study, the temperature range of the decomposition of Dawsonite is at about 300-400°C, a result that is consistent with the bibliography. Any differences between the study and the bibliography lie, again, in the different conditions of every study.

Chapter 8 – Summary, Conclusion, Recommendation

The crystalline structure and the crystalline phases that are present in Huntite-Hydromagnesite, Brucite and Dawsonite, have been well defined. Their thermal decomposition at different experimental conditions have been well characterized.

In comparison to ATH, the widely used fire retardant, all three minerals studied start to decompose at a higher temperature. Alumina trihydrate starts to decompose at about 200°C, with a major mass loss at approximately 300°C and is fully decomposed at about 350°C [5, 6].

Specifically, the mixture of Huntite-Hydromagnesite has a wide endothermic decomposition that provides cooling at a wider temperature range than the aluminum hydroxide [15], since Hydromagnesite starts to decompose at about 250°C and Huntite completes decomposition at about 800°C. The sample studied, shows a major mass loss at approximately 585°C. Nonetheless, for the sample to be more efficient, a 50:50 mixture of Huntite and Hydromagnesite is recommended. In that way, the sample will cover a wider temperature range, allowing higher processing temperature.

Also, Brucite is already being used as a fire-retardant filler in the current fire-retardant industry. However, the sample studied here needs to have a higher content in $Mg(OH)_2$, preferably about 90% for a greater beneficiation. Since it has a thermal decomposition temperature range of approximately 350-500°C, with a major mass loss at approximately 428°C, it is suitable for materials with higher processing temperatures than those where ATH is applied to.

Moreover, Dawsonite seems to be the most competitive mineral of the three studied, compared to ATH, since it starts to decompose at approximately 300°C. A major mass loss occurs at about 376°C, a temperature which is very close to the point of infliction of the ATH.

In conclusion, with the data obtained from this study, the decomposition temperature of Dawsonite is the closest one to the decomposition temperature of ATH, compared to the other two samples.

References

1. Troitzsch, J.H., *Overview of flame retardants, fire and fire safety, markets and applications, mode of action and main families, role in fire gases and residues.* Chimica Oggi/chemistry Today, 1998. **16**: p. 18-24.
2. Bourbigot, S., et al., *Fire Retardancy of Polymers: New Applications of Mineral Fillers.* The Royal Society of Chemistry, 2005. **14**: p. 189-201.
3. Rothon, R., *Mineral requirements for flame retardants.* Industrial Mineral, 1994.
4. Kirschbaum, G.S. *Flame retardant minerals - Markets and technology*. in *12th Industrial Minerals International Congress*. 1996. Chicago, IL.
5. Huber, *Non-halogen fire retardant additives*.
6. Mettler-Toledo, *TGA of Aluminum Trihydrate and Magnesium Hydroxide*.
7. Calvo, J.P., M.G. Stamatakis, and A. Magganas, *Clastic huntite in upper Neogene formations of the Kozani Basin, Macedonia, northern Greece.* Journal of Sedimentary Research, 1995. **65**(4a): p. 627-632. https://doi.org/10.1306/D426817B-2B26-11D7-8648000102C1865D %J Journal of Sedimentary Research
8. Stamatakis, M.G., *Occurrence and genesis of huntite-hydromagnesite assemblages, Kozani, Greece - important new white fillers and extenders.* TRANSACTIONS- INSTITUTION OF MINING AND METALLURGY, 1995. **104**(b).
9. Inglethorpe, S.D. and M.G. Stamatakis, *Thermal decomposition of natural mixtures of hydromagnesite and huntite from Kozani, Northern Greece.* Mineral Wealth, 2003. **126**: p. 7--18.
10. *Kuldur deposit.* Available from: http://en.magminerals.ru/about/minefield/.
11. Ferrini, V., et al., *The Koman dawsonite and realgar-orpiment deposit, Northern Albania: Inferences on processes of formation.* The Canadian Mineralogist, 2003. **41**: p. 413-427. https://doi.org/10.2113/gscanmin.41.2.413
12. Skoog, D.A., F.J. Holler, and S.R. Crouch, *Principles of Instrumental Analysis.* 7th ed. 2017: Cengage Learning.
13. Hollingbery, L.A. and T.R. Hull, *The fire retardant behaviour of huntite and hydromagnesite – A review.* Polymer Degradation and Stability, 2010. **95**(12): p. 2213-2225. https://doi.org/10.1016/j.polymdegradstab.2010.08.019
14. Liu, C., T. Liu, and D. Wang, *Non-isothermal kinetics study on the thermal decomposition of brucite by thermogravimetry.* Journal of Thermal Analysis and Calorimetry, 2018. **134**(3): p. 2339-2347. https://doi.org/10.1007/s10973-018-7654-4
15. Hollingbery, L.A. and T.R. Hull, *The thermal decomposition of huntite and hydromagnesite—A review.* Thermochimica Acta, 2010. **509**(1): p. 1-11. https://doi.org/10.1016/j.tca.2010.06.012
16. Földvári, M., *Handbook of Thermogravimetric System of Minerals and Its Use in Geological Practice*. 2011, Budapest: Geological Institute of Hungary (=Magyar Állami Földtani Intézet).
17. Walter, M.D. and M.T. Wajer, *Overview of Flame Retardants Including Magnesium Hydroxide.* Martin Marietta Magnesia Specialties, LLC, 2015.
18. Smith, J.W. and N.B. Young. *Dawsonite: its geochemistry, thermal behavior, and extraction from Green River oil shale*. 1975. United States.